15-9-1992

Magneto-optical probe of two-dimensional electron liquid and solid phases

E. M. Goldys
University of New South Wales

S. A. Brown
University of New South Wales

R. B. Dunford
University of New South Wales

A. G. Davies
University of New South Wales

R. Newbury
University of New South Wales

See next page for additional authors

RAPID COMMUNICATIONS

PHYSICAL REVIEW B VOLUME 46, NUMBER 12 15 SEPTEMBER 1992-II

Magneto-optical probe of two-dimensional electron liquid and solid phases

E. M. Goldys, S. A. Brown, R. B. Dunford, A. G. Davies, R. Newbury, and R. G. Clark
School of Physics, University of New South Wales, P.O. Box 1, Kensington 2033, Australia

P. E. Simmonds
Department of Physics, University of Wollongong, P.O. Box 1144, Wollongong 2500, Australia

J. J. Harris
Interdisciplinary Research Centre for Semiconductor Materials, University of London, Prince Consort Road, London SW7 2BZ, United Kingdom

C. T. Foxon
Department of Physics, University of Nottingham, University Park, Nottingham NG7 2RD, United Kingdom
(Received 6 July 1992)

Band-gap photoluminescence (PL) is used to establish the optical signature of a GaAs-$Ga_{1-x}Al_xAs$ heterojunction in the extreme quantum limit. The temperature and field dependence of new PL structure maps a phase boundary which correlates with the electron liquid-solid transition.

Following the discovery of the fractional quantum Hall effect (FQHE) in a two-dimensional electron system (2DES), there have been a number of investigations designed to observe the electron liquid-solid (Wigner crystal) phase transition. Wigner crystallization is predicted below a critical Landau-level filling factor ν_c at high magnetic fields and low temperatures.[1] Experimental reports, for high-quality GaAs-$Ga_{1-x}Al_xAs$ heterostructures, include measurements of sample resistivity,[2] nonlinear *I-V* characteristics,[3-6] radio frequency (rf) absorption,[5,7] surface acoustic wave (SAW) attenuation,[8] and cyclotron resonance (CR).[9]

Recently, there has been intense interest in experiments that probe both FQHE states[10-17] and the condensed Wigner solid phase[12,13,15-18] of the 2DES by magneto-photoluminescence (PL) at low temperatures. The optical experiments fall into two categories, resulting from important structural differences in the samples studied which determine the PL recombination process: 2D electron–free valence hole (*e-h*) (Refs. 10, 11, 13, 14, 16, and 17) and 2D electron–acceptor-bound hole (e-A^0).[12,15,18] Where recombination involves holes confined to a Be δ-doped layer (e-A^0), a strong signal associated with the Wigner solid has been observed in addition to steps in PL energy associated with FQHE energy gaps.[12,15] In contrast, no definitive optical signal[19] has been associated with the Wigner solid in standard single heterojunction (SHJ) samples, used in all other work,[2-9] where recombination involves only valence-band holes (*e-h*). For the standard structures, energy shifts and strong PL intensity variations have been observed at FQHE states which exhibit major differences with data from δ-doped samples. It is clear from these experiments that the nature and location of the holes in the two types of sample is of central importance, but a theoretical understanding is only now emerging for the FQHE (Ref. 20) and no theory exists for the Wigner regime. It is therefore important to establish the optical signature of the Wigner solid in standard samples.

In this paper, we report *e-h* PL measurements in a high-quality, low-density SHJ. We observe an intense spectral feature in the low-ν limit, the temperature and field dependence of which is used to define two characteristic temperatures, T_{c1} and T_{c2}. We find that the boundary formed by the lower, T_{c1}, mapping is strongly correlated with the liquid-solid transition.

PL measurements at an excitation wavelength of 740 nm, at temperatures down to 70 mK and magnetic fields to 15.5 T, have been carried out in a GaAs-$Ga_{1-x}Al_xAs$ SHJ, sample G648 (saturated $n_s = 3.2\times10^{10}$ cm^{-2}, $\mu \sim 3\times10^6$ cm^2/V s) with a large $Ga_{1-x}Al_xAs$ spacer layer (4800 Å). The sample was mounted in the dilute phase of a ^{3}He/^{4}He refrigerator. Optical fibers delivered light from a Ti-sapphire laser and PL was collected using a triple spectrometer with a cooled charge-coupled device array. Low laser powers at the sample (2D layer 2.5×2.5 mm^2) in the range 0.025–0.5 μW were used to eliminate electron heating. Simultaneous transport measurements showed sharp FQHE structure out to $\nu = \frac{1}{5}$. Under prolonged illumination some parallel photoconductivity was observed; this had no effect on the PL spectra over our magnetic field range.

Figure 1 illustrates the magnetic field dependence of the PL spectra at 70 mK and 2.2 K. The evolution of PL peak intensities at 70 mK is presented in Fig. 2: (a) $B = 0$ to 2.8 T, (b) $B = 2.8$ to 5 T, and (c) $B > 5$ T. Filling factors obtained from simultaneous transport measurements are marked by vertical lines in Fig. 2; lines at $\nu = \frac{1}{7}$ and $\frac{1}{9}$ are inferred from FQHE structure $\nu \geq \frac{1}{5}$. In Fig. 2(a) (integer QHE and $\frac{2}{3}$ FQHE hierarchy), two sharp PL lines are observed (Fig. 1) corresponding to recombination between the $l_e = 0$ Landau level of the E_0 and E_1 electron subbands and the lowest-energy hole Landau level. For $B < 0.8$ T, higher Landau levels of the 2DES are observed in the E_0 emission (not shown). The characteristic intensity modulations (minima in E_0, maxima in E_1 at QHE states) have been explained by correlation and screening effects.[10,11,14,16,17] In Fig. 2(b) ($\frac{1}{3}$ FQHE

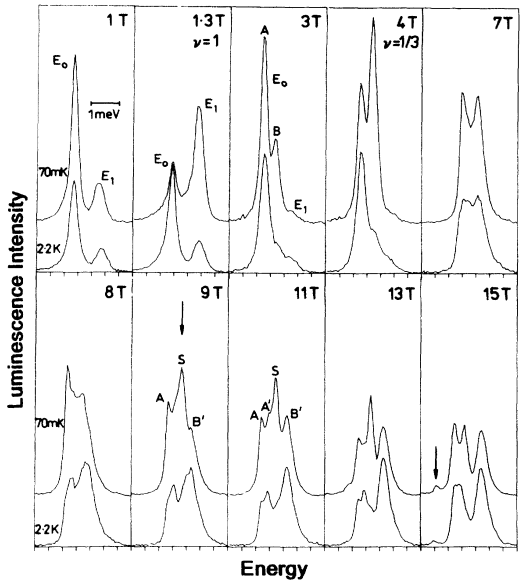

FIG. 1. Field dependence of (e-h) PL spectra at 70 mK and 2.2 K. Intensity in arbitrary units.

hierarchy), a doublet structure labeled A,B emerges. Figure 3 shows the PL transition energies; the trajectory of the A line extends on smoothly from the E_0 (singlet) emission discussed above, while the B line is higher in energy by $\sim$0.5 meV and lies between the E_0 and E_1 data. The PL spectrum at 3 T in Fig. 1 captures the emergent B peak as structure additional to the E_1 line, which becomes barely detectable beyond this field. The origin of the B line is not understood, but doublet structure in the region of the $\frac{1}{3}$ FQHE hierarchy, of a magnitude similar to the A-B splitting, has been observed in other SHJs (Refs. 13 and 16) and in the E_0 emission of single quantum wells.[14] It is clear from Fig. 1 that the B peak is significantly weaker than the A peak at 2.2 K, whereas at 70 mK they are comparable. Intensity minima in the A line in Fig. 2(b) correlate well with $\nu=\frac{1}{3}$, $\frac{2}{5}$, $\frac{3}{7}$ states of the $\frac{1}{3}$ hierarchy, consistent with the optical signature established for the $\frac{2}{3}$ hierarchy.[10,11] This important symmetry was not observed in earlier work.[13] Additionally, intensity minima in the A line correlate with maxima in the B line. While this is analogous to E_0,E_1 behavior at FQHE states of the $\frac{2}{3}$ hierarchy, the mechanism may well be different; if the B line is associated with the E_0 subband, competition for recombination with holes is relevant.

The most important change in the PL is observed at 70 mK in the low-ν limit where a dramatic breakup of the A,B doublet to a complex structure labeled A,S,B' in Figs. 1–3 occurs, dominated by the new, central S peak (shown by an arrow in Fig. 1 at 9 T). In addition, structure close to the A line, labeled A' in Fig. 1 [corresponding to ◇ data in Figs. 2(c) and 3], is intermittently resolved over the region 7–14 T. A similar complex breakup in a higher density sample[13] could not be investigated in detail for $\nu \ll \frac{1}{5}$ due to the available magnetic field range. Significantly, a weak low-energy peak (shown by an arrow in Fig. 1 at 15 T) is also observed above 12 T [$\nu < \frac{1}{9}$, ◆ data in Figs. 2(c) and 3] split off from the main E_0 emission by 0.65 meV at 15 T. This latter feature is reminiscent of the low-energy peak observed for $\nu < 0.28$ in δ-doped structures[12] attributed to a solid phase, and a low-energy shoulder recently reported in a standard SHJ (Ref. 16) in the region $\nu < 0.21$. In Fig. 3, a careful examination of the spectral evolution in the range 7–9 T reveals that S and B' do not obviously emerge from B; the energy trajectory of the S line is lower in energy by $\sim$0.1 meV and our interpretation is that the B peak falls in intensity with the onset of new S (and B') structure. It is difficult to determine a precise threshold field for the S peak, but the collapse in B intensity sets in close to $\nu=\frac{2}{9}$; see Figs. 2(b) and (c). The emergence of S structure is also accompanied by a falloff in *total* integrated intensity close to $\nu=\frac{1}{5}$ (Fig. 3, inset); a similar falloff occurs in Be δ-doped samples[12] and other SHJs.[16]

In the extreme quantum limit, the S peak, which dominates the 70 mK spectrum is not resolved above $\sim$2 K (Fig. 1). This remarkable temperature dependence is highlighted in Fig. 4(a); the spectral weight is transferred from S to B' on raising the temperature. This behavior, coupled with the onset of S structure at high field, strongly suggests that it can be used to map out a phase boundary in the (B,T) plane.

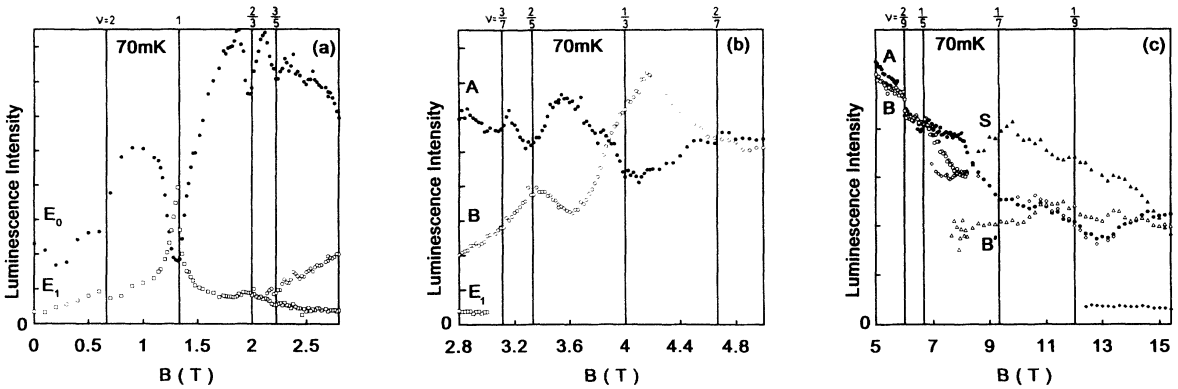

FIG. 2. PL intensity data in arbitrary units at 70 mK for (a) integer QHE and $\nu=\frac{2}{3}$ FQHE hierarchy, (b) $\nu=\frac{1}{3}$ FQHE hierarchy, and (c) extreme quantum limit—note the scale change.

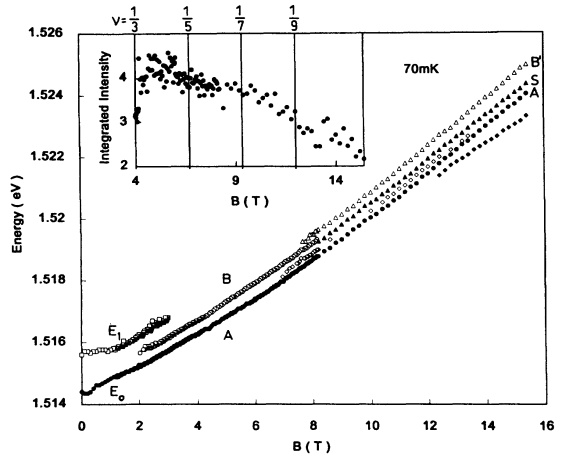

FIG. 3. PL energy data at 70 mK. Inset: Total integrated PL intensity, in arbitrary units.

The emergent S structure has been studied systematically and analyzed by plotting the peak height ratio S/B', similar to the procedure of Ref. 12. Representative S/B' data over the temperature range 0.1–3.5 K, at 9.24 and 12.5 T, are shown in Fig. 4(b); fitted lines define two characteristic temperatures, T_{c1} and T_{c2}, below and above which (respectively) the ratio S/B' shows little change. The low-temperature regions are expanded in the Fig. 4(b) insets. While T_{c1} is well defined, the ratio change in the vicinity of T_{c2} is less abrupt; the definition of T_{c2}, by the intersection of the extrapolated high-temperature saturation value of S/B' with the straight-line fit through the steep rise between T_{c1} and T_{c2}, is adopted as a reasonable criterion to characterize the onset of the rise. Plots of alternative ratios such as S/A, S/A', $S/(A+A'+B')$ have a similar but less abrupt form to Fig. 4(b), but are consistent with T_{c1}, T_{c2} values obtained from S/B'. The analogous procedure to determine an onset field B_c at fixed temperature is difficult, due to the complexity of the spectral evolution in the transition region 7–9 T (Fig. 1); below 8 T the S peak is masked by the strong adjacent PL structure and the expected continuous falloff in S intensity to lower fields cannot be tracked. We limit the analysis to T_{c1} data (● and ▼ distinguish two different runs) and T_{c2} data (○,▽) plotted as reduced temperatures $t = T/T_{cm}$ vs ν in Fig. 5. T_{cm} is the classical 2D melting temperature of the electron solid; $T_{cm} = \Gamma^{-1} e^2/4\pi\varepsilon\varepsilon_0 k_B a$ with $\Gamma = 127$ and $a = (\pi n_s)^{-1/2}$.

T_{c1}, T_{c2} values from our measurements of electron-*valence-band hole* PL are compared in Fig. 5 with optical data for electron-*neutral acceptor* transitions in Be δ-doped structures.[12,15,18] For e-A^0 PL,[12] in addition to a line present throughout the magnetic field range studied (I_1), a new line (I_2) was observed at lower energy for $\nu < 0.28$. I_1 and I_2 were attributed to electron liquid and solid phases, respectively. A transition temperature was deduced from discontinuities in intensity ratio plots I_2/I_1, denoted ♦ in Fig. 5. Recently two thresholds have been observed in this work,[15] denoted ■ and ▲, analogous but not identical to our T_{c1} and T_{c2} (I_2 intensity exhibits a different characteristic than our S peak). The two thresholds are discussed as a two-step transition from liquid to solid.[15] The upper dashed line in Fig. 5 is from more extensive measurements[18] of the higher temperature transition in the same δ-doped samples which, in this interpretation, shows reentrant liquid states[12] close to $\nu = \frac{1}{5}$ and $\frac{1}{7}$.

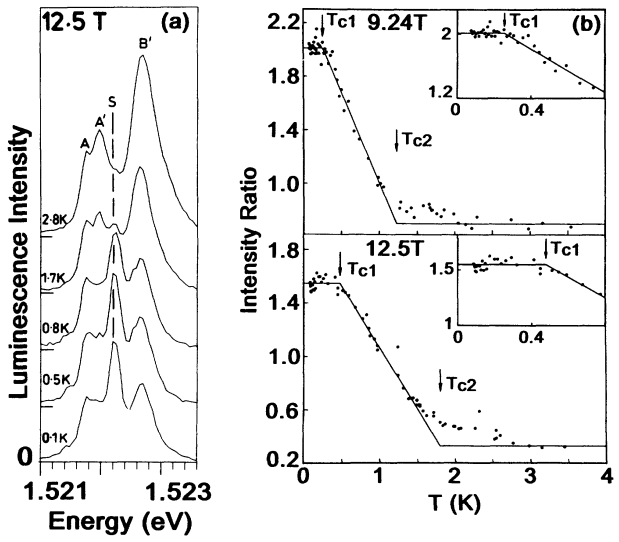

FIG. 4. (a) Temperature dependence of high-field PL structure. (b) Ratio of peak intensities S/B', defining critical temperatures T_{c1} and T_{c2}.

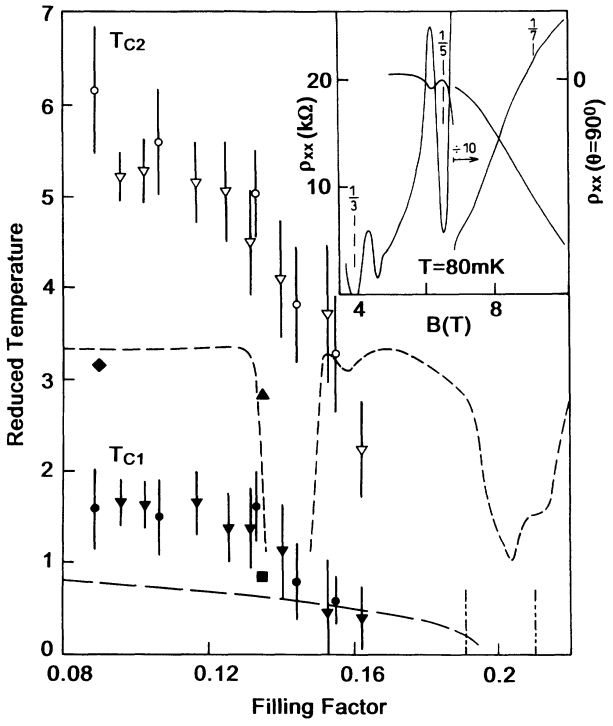

FIG. 5. Phase diagram established from the Fig. 4(b) analysis of (e-h) PL. T_{c1} and T_{c2} data are compared with previous reports for the liquid-solid transition—see text. Inset: Low-temperature ρ_{xx} data.

Also shown in Fig. 5 is the upper limit of a phase boundary from rf absorption and threshold *I-V* for a Wigner crystal broken into pinned domains (lower dashed line);[5] this agrees well with other *I-V* data[4] and in the region of overlap ($\nu=0.14$–0.19) with an onset boundary from SAW data, interpreted as the pinning mode of the Wigner crystal.[8] At lower ν, the Ref. 5 boundary is also in broad agreement with recent CR measurements.[9] The two vertical dashed lines in Fig. 5 mark the extent of the $\nu=\frac{1}{5}\rho_{xx}$ minimum in our sample. Characteristic ρ_{xx} data, taken before the onset of parallel photoconductivity, are shown in the Fig. 5 inset ($n_s=3.1\times10^{10}$ cm^{-2}). An important feature is the abrupt onset of a ρ_{xx} out-of-phase component ($\theta=90°$) for $\nu<\frac{1}{5}$, and to a lesser extent between $\nu=\frac{2}{9}$ and $\frac{1}{5}$, that has been linked to threshold conduction for a pinned Wigner solid.[5]

One interpretation of the complex *e-h* spectra shown in Fig. 1 at lowest ν, is that the split-off low-energy peak (arrowed at 15 T) and the *A* line are analogous to the (e-A^0) I_2,I_1 peaks observed in the δ-doped samples. An analysis of the temperature-dependent intensity of our low-energy peak at 15 T, as in Fig. 4(b), yields a T_{c1} in good agreement with the S/B' analysis. The situation in standard SHJs is complicated, however, by the higher-energy *B* and E_1 lines at lower fields, which might result in an *additional* S,B' pairing that is also analogous to I_2, I_1. This interpretation is reinforced by the similar splittings of these pairs shown in Fig. 3; the energy trajectories of the split-off peak and *A* extrapolate back to a convergence close to $\nu=\frac{1}{5}$ as do the S,B' trajectories. However, the origin of this PL structure is not known and other scenarios are possible.

The most important observation from Fig. 5 concerns T_{c1}. The phase boundary determined from our measurements of *e-h* PL, and the single data point (■) from e-A^0 PL in δ-doped samples, are in reasonable agreement. Our T_{c1} values define a boundary which agrees well with CR data[9] at $\nu=0.09$ and 0.11; 90% occupancy of the solid phase was deduced at $T\sim400$ mK with $T_{cm}=310$ mK, corresponding to $t=1.29$. The lower limit of our T_{c1} boundary is ~50% higher in temperature at the lowest filling factor studied ($\nu=0.09$) than that obtained from rf absorption and threshold conduction,[5] itself consistent with SAW data.[8] While the association of T_{c1} with solidification has a good experimental basis, our T_{c2} data and the e-A^0 second threshold (Fig. 5 upper dashed line, ◆ and ▲ data) differ substantially, notwithstanding differences in the samples or definitions of these critical temperatures. This places less physical significance on T_{c2} as an absolute measurement for the onset of an intermediate phase[15] and is supported by CR data,[9] where structure attributed to coexisting liquid and solid extends to remarkably high temperatures (~10 K). T_{c2} may depend on the extent of nonlinearity of the optical probe to the degree of solidification.

In conclusion, we have presented comprehensive data that establishes the optical signature of a standard SHJ in the extreme quantum limit. A phase boundary is established from electron–valence hole PL that is situated close to the electron liquid-solid phase transition mapped out in similar samples by a variety of techniques.

[1]P. K. Lam and S. M. Girvin, Phys. Rev. B **30**, 473 (1984); D. Levesque, J. J. Weis, and A. H. MacDonald, *ibid.* **30**, 1056 (1984).

[2]H. W. Jiang, R. L. Willett, H. L. Störmer, D. C. Tsui, L. N. Pfeiffer, and K. W. West, Phys. Rev. Lett. **65**, 633 (1990).

[3]R. L. Willett, H. L. Störmer, D. C. Tsui, L. N. Pfeiffer, K. W. West, and K. W. Baldwin, Phys. Rev. B **38**, 7881 (1988); R. L. Willett, H. L. Störmer, D. C. Tsui, L. N. Pfeiffer, K. W. West, M. Shayegan, M. Santos, and T. Sajoto, *ibid.* **40**, 6432 (1989).

[4]V. J. Goldman, M. Santos, M. Shayegan, and J. E. Cunningham, Phys. Rev. Lett. **65**, 2189 (1990).

[5]F. I. B. Williams, P. A. Wright, R. G. Clark, E. Y. Andrei, G. Deville, D. C. Glattli, O. Probst, B. Etienne, C. Dorin, C. T. Foxon, and J. J. Harris, Phys. Rev. Lett. **66**, 3285 (1991).

[6]Y. P. Li, T. Sajoto, L. W. Engel, D. C. Tsui, and M. Shayegan, Phys. Rev. Lett. **67**, 1630 (1991).

[7]E. Y. Andrei, G. Deville, D. C. Glattli, F. I. B. Williams, E. Paris, and B. Etienne, Phys. Rev. Lett. **60**, 2765 (1988).

[8]M. A. Paalanen, R. L. Willett, P. B. Littlewood, R. R. Ruel, K. W. West, L. N. Pfeiffer, and D. J. Bishop (unpublished).

[9]G. M. Summers, M. Watts, R. A. Lewis, R. J. Nicholas, J. J. Harris, and C. T. Foxon (unpublished).

[10]A. J. Turberfield, S. R. Haynes, P. A. Wright, R. A. Ford, R. G. Clark, J. F. Ryan, J. J. Harris, and C. T. Foxon, Phys. Rev. Lett. **65**, 637 (1990).

[11]B. B. Goldberg, D. Heiman, A. Pinczuk, L. Pfeiffer, and K. West, Phys. Rev. Lett. **65**, 641 (1990).

[12]H. Buhmann, W. Joss, K.v. Klitzing, I. V. Kukushkin, G. Martinez, A. S. Plaut, K. Ploog, and V. B. Timofeev, Phys. Rev. Lett. **65**, 1056 (1990); **66**, 926 (1991).

[13]R. G. Clark, R. A. Ford, S. R. Haynes, J. F. Ryan, A. J. Turberfield, P. A. Wright, C. T. Foxon, and J. J. Harris, *High Magnetic Fields in Semiconductor Physics III,* edited by G. Landwehr, Springer Series in Solid State Sciences Vol. **101** (Springer-Verlag, Berlin, 1992), p. 231.

[14]B. B. Goldberg, D. Heiman, A. Pinczuk, L. Pfeiffer, and K. West, in *High Magnetic Fields in Semiconductor Physics III* (Ref. 13), p. 243.

[15]I. V. Kukushkin, N. J. Pulsford, K.v. Klitzing, K. Ploog, R. J. Haug, S. Koch, and V. B. Timofeev, Surf. Sci. **263**, 30 (1992); Phys. Rev. B **45**, 4532 (1992).

[16]B. B. Goldberg, D. Heiman, A. Pinczuk, L. Pfeiffer, and K. West, Surf. Sci. **263**, 9 (1992).

[17]A. J. Turberfield, S. R. Haynes, P. A. Wright, R. A. Ford, R. G. Clark, J. F. Ryan, J. J. Harris, and C. T. Foxon, Surf. Sci. **263**, 1 (1992).

[18]M. Hayne, M. K. Ellis, A. S. Plaut, A. Usher, and K. Ploog, Surf. Sci. **263**, 39 (1992).

[19]References 13, 16, and 17 identified two candidates for signatures of a solid phase, but detailed studies were not performed.

[20]V. M. Apal'kov and E. I. Rashba, Pis'ma Zh. Eksp. Teor. Fiz. **53**, 420 (1991) [JETP Lett. **53**, 442 (1991)]; A. H. MacDonald, E. H. Rezayi, and D. Keller, Phys. Rev. Lett. **68**, 1939 (1992).